J Supercond Nov Magn (2017) 30:2239–2245
DOI 10.1007/s10948-017-4024-6

ORIGINAL PAPER

Investigation of Electromagnetic Properties of La-Doped Strontium Ferrite in X and Ku Bands

Pawandeep Kaur[1] · S. Bindra Narang[1] · Shalini Bahel[1]

Received: 9 December 2016 / Accepted: 20 February 2017 / Published online: 8 March 2017

Abstract In the present study, the lanthanumsubstituted strontium ferrite particles with general formula, $Sr_{1-x}La_xFe_{12}O_{19}$ ($x = 0$, 0.10, 0.15, 0.20, and 0.25) were prepared using citrate auto-combustion method. These ferrites were characterized by X-ray diffraction (XRD), scanning electron microscope (SEM), vibrating sample magnetometer (VSM), and vector network analyzer (VNA). X-ray diffraction patterns show the formation of M-type hexaferrite phase without any secondary phases for all the synthesized samples. The complex permittivity ($\varepsilon'-j\varepsilon''$) and complex permeability ($\mu'-j\mu''$) were measured using VNA in X-band (8.2–12.4 GHz) and Ku-band (12.4–18 GHz) frequency range at room temperature. More than 90 % absorption was obtained in the Ku band for all the La^{3+}substituted strontium ferrites. The composition $x = 0.15$ exhibits a minimum reflection loss of −20.66 dB at 16.5 GHz and an absorption bandwidth of 2.1 GHz (15.63 to 17.64 GHz) with an absorber layer thickness of 1.6 mm. These materials can be used as cost-effective and thinlayer microwave absorbers in higherfrequency range.

Keywords Strontium ferrite · Hysteresis · Tangent loss · Microwave absorption

✉ S. Bindra Narang
sukhleen2@yahoo.com

[1] Department of Electronics Technology,
Guru Nanak Dev University, Amritsar, India

1 Introduction

The electromagnetic interference (EMI) poses serious problems due to rapid development of high-speed electronic circuits at microwave frequency range. M-type hexagonal ferrites can be used as microwave absorber owing to its large magnetocrystalline anisotropy [1]. The hexagonal ferrites can be engineered to find application as absorber at microwave frequencies. Many researchers have reported the use of hexagonal ferrites as radar-absorbing material (RAM) and EMI suppression materials [2, 3].

The conventional process to synthesize strontium ferrite requires sintering at high temperature thereby increasing its cost. As a consequence, a large number of low-temperature methods, such as sol-gel [4], co-precipitation [5], and hydrothermal method [6], have been developed to control the shape and size of the particles and the properties of the material. The substitution of a small amount of divalent and tetravalent ions in strontium ferrite modifies its magnetic and electro-magnetic properties [7, 8]. It has been reported that the rare earth element acts as an inhibiting agent for grain growth and shows a modification in magnetic properties [9]. A suitable amount of La^{3+} ion substitution in M-type [10] and W-type [11] ferrites can improve the microwave absorption properties. The present work deals with the synthesis of $Sr_{1-x}La_xFe_{12}O_{19}$ ($x = 0$, 0.10, 0.15, 0.20, and 0.25) ferrite by the citrate auto-combustion method. Using this method, it is possible to obtain submicron particles for achieving useful properties for practical materials. Electromagnetic properties and microwave absorbing characteristics of synthesized La-substituted M-type strontium ferrite have been studied.

2 Experimental

2.1 Synthesis of Ferrites

The La-substituted strontium ferrite particles with general formula, $Sr_{1-x}La_xFe_{12}O_{19}$ ($x = 0$, 0.10, 0.15, 0.20, and 0.25) were prepared by citrate auto-combustion method. The stoichiometric amounts of metal nitrates were used as per (1):

$$(1-x)\,(\mathrm{Sr}\,(\mathrm{NO_3})_2) + x\left(\mathrm{La}\,(\mathrm{NO_3})_3 \cdot 6\mathrm{H_2O}\right) + \left(\mathrm{Fe}\,(\mathrm{NO_3})_3 \cdot 9\mathrm{H_2O}\right) \xrightarrow[\text{Mixing, dehydration, and combustion}]{\text{Citric acid}} \mathrm{Sr_{1-x}La_xFe_{12}O_{19}} \quad (1)$$

Desired metal nitrates in appropriate ratios were taken in minimum amount of distilled water, and the aqueous solution of citric acid was added. Ammonia solution was then added to adjust the pH to 7.0. The solution was slowly evaporated at 80 ° C until a brown gel was formed. Prepared dry gels were heated in the air at 220°C to invoke ignition. Auto-combustion occurred, and a dry fluffy mass was obtained. Finally, this precursor powder was calcinated at 1100°C for 5 h in a muffle furnace where the heating rates were maintained at 5°C/min. The material was allowed to cool naturally and compressed at 8 tons to make pellets.

2.2 Measurement of Properties

The electromagnetic properties were studied by using Agilent N5225A vector network analyzer. The synthesized pellets were shaped to fit exactly into 22.86 × 10.16 and 15.79 × 7.89 mm^2 rectangular X-band (WR-90) and Ku-band (WR-62) waveguide flanges, respectively. A full two-port calibration was initially done on the test setup in order to remove errors due to source/load match, isolation, etc. The complex permittivity ($\varepsilon' - j\varepsilon''$) and permeability ($\mu' - j\mu''$) were then determined from the measured scattering parameters using Agilent software module 85071 in the frequency range of 8.2–18 GHz at room temperature.

Hysteresis measurements of all the samples at room temperature in the field range of ±15 kOe were carried out by a vibrating sample magnetometer (Microsense-Model 10). XRD patterns were obtained by using a diffractometer (Panalytical X'pert pro) with CuKα radiation ($\lambda = 1.5406$ Å). Scanning electron microscope (Zeiss-Supra 55) was used to investigate the morphology of the hexaferrites.

3 Results and Discussion

XRD patterns of $Sr_{1-x}La_xFe_{12}O_{19}$ ($x = 0.0$, 0.10, 0.15, 0.20, and 0.25) recorded at room temperature are presented in Fig. 1. All the diffraction peaks are indexed according to the standard of the American Society for Testing and Materials (JCPDS file number 33-1340). XRD analysis has confirmed the formation of M-type hexagonal structures in all the synthesized samples. The lattice constants a and c were calculated from the value of $d_{(hkl)}$ corresponding to (110), (107), and (114) planes according to the formula given by (2) [12];

$$D_{(hkl)} = 4/3 \times \left(\left(\left(h^2 + hk + k^2\right)\Big/ a^2\right) + l^2\Big/c^2\right)^{-1/2} \quad (2)$$

The lattice parameters, a and c were observed to increase as x increased from 0.0 to 0.15 and then decreased at higher values of x. These changes in lattice parameters may be attributed to differences in ionic radii of Sr^{2+} and La^{3+} ions. La^{3+} (1.36 Å) ion being smaller than Sr^{2+} ion (1.44 Å) could be well accommodated at the Sr^{2+} site and some Fe^{3+} ions converted into Fe^{2+} ions in order to compensate the excess positive charges due to the replacement of Sr^{2+} by La^{3+} [10], which contributes to the lattice expansion. At composition $x = 0.20$, lattice parameter decreased which may be attributed to lattice contraction as the size effect overtakes the charge neutrality effect. The unit cell volume variation corresponds to the change in bulk density (experimental). The M-type hexagonal structure is retained as the observed c/a parameter for all the synthesized samples is lower than 3.98 [13], as shown in Table 1. The average crystallite sizes (D) of all the samples were calculated from the highest-intensity (107 and 114) peaks of XRD patterns by using Debye-Scherrer formula, given by (3) [14].

$$D = K\lambda/(\beta\cos\theta) \quad (3)$$

where β is the broadening of diffraction lines at half of its maximum intensity, λ is the wavelength ($\lambda = 1.5406$ Å), θ is the Bragg angle, and K is the shape factor that is equal to 0.89 for hexaferrites. The crystallite sizes were in the range of 34.3–42.56 nm (Table 1).

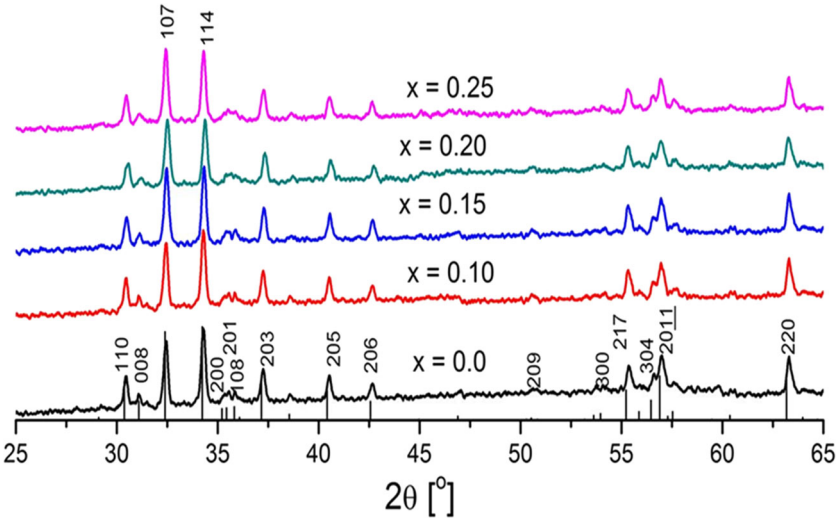

Fig. 1 X-ray diffraction patterns of $Sr_{1-x}La_xFe_{12}O_{19}$ ($x = 0.0$, 0.10, 0.15, 0.20, and 0.25) ferrites

The SEM micrographs of all the synthesized ferrite samples are shown in Fig. 2. The particles seem to have spherical shaped morphology for all compositions. The average SEM grain diameter (D_m) decreases from 187 to 148 nm with lanthanum substitution from $x = 0.00$ to 0.10, respectively. The average grain diameter with further substitution of lanthanum in strontium ferrite increases from 148 nm for $x = 0.10$ to 180 nm for $x = 0.25$ sample (Table 2).

The magnetic hysteresis loops for $Sr_{1-x}La_xFe_{12}O_{19}$ ($x = 0.0$, 0.10, 0.15, 0.20, and 0.25) ferrites are shown in Fig. 3. The values of saturation magnetization (M_s), coercivity (H_c), remanence (M_r), and magnetocrystalline anisotropy (H_a) are obtained from hysteresis data and are summarized in Table 2. The results indicate a high level of magnetic characteristics of strontium ferrite samples. The saturation magnetization value for $x = 0.0$ sample is 65.36 emu/g and coercivity is 5059 Oe. The value of net magnetization decreases from 62.3 to 57.85 emu/g, and the coercivity decreases from 5791 to 5661 Oe, respectively, with an increase in the amount of doping of La^{3+} ion from $x = 0.10$ to 0.25. The squareness ratio (M_r/M_s) greater than 0.5 for all the compositions suggests that the prepared ferrites have randomly oriented domain particles [15].

A wide variation in intrinsic coercivity range 5791 to 5661 kOe has been obtained upon substitution but still lower than the theoretically estimated limit of H_c (7400 Oe) [16, 17]. It is well known that the coercivity depends on crystallite size and magnetocrystalline anisotropy. The axis of magnetization is parallel to hexagonal c-axis, described by anisotropy constant K_1, and different sites contribute differently to the magnetic anisotropy. H_c value increases by 12–14 % with La^{3+} substitution in strontium ferrite which may be due to the increase in H_a. The coercivity decreases with increase in concentration of La^{3+} ions in strontium ferrite which follows a trend similar to that of the H_a constant. Another reason for reduction in coercivity is extrinsic effect which causes an increase in grain diameter from 148 to 180 nm with lanthanum substitution from $x = 0.10$ to 0.25, respectively. This effect can be attributed to coercivity which is inversely related to the grain diameter [18, 19].

The variation of ε', ε'', μ', and μ'' for $Sr_{1-x}La_xFe_{12}O_{19}$ ($x = 0.0$, 0.10, 0.15, 0.20, and 0.25) with frequency are shown in Fig. 4. From Fig. 4a, b, it can be seen that the real and imaginary parts of the permittivity show a good dispersion with the increase in frequency. The ε' values increase with increase in La^{3+} substitution except for the

Table 1 Variation of hexagonal lattice parameters (a and c), cell volume (V), and crystallite size (D), bulk density (ρ_b), X-ray density (ρ_x), and porosity with La substitution in Sr ferrite

x	0	0.1	0.15	0.2	0.25
a (Å)	5.8837	5.8841	5.8857	5.8792	5.8844
c (Å)	23.032	23.038	23.041	23.026	23.033
c/a	3.9145	3.9153	3.9147	3.9165	3.9142
V (Å3)	690.51	691.23	691.24	689.27	690.71
D (nm)	42.56	34.3	39.21	36.81	40.54
ρ_b (gcm^{-3})	2.6	2.62	2.74	2.64	2.57
ρ_x (gcm^{-3})	4.84	4.86	4.87	4.9	4.9
Porosity	0.462	0.46	0.437	0.461	0.47

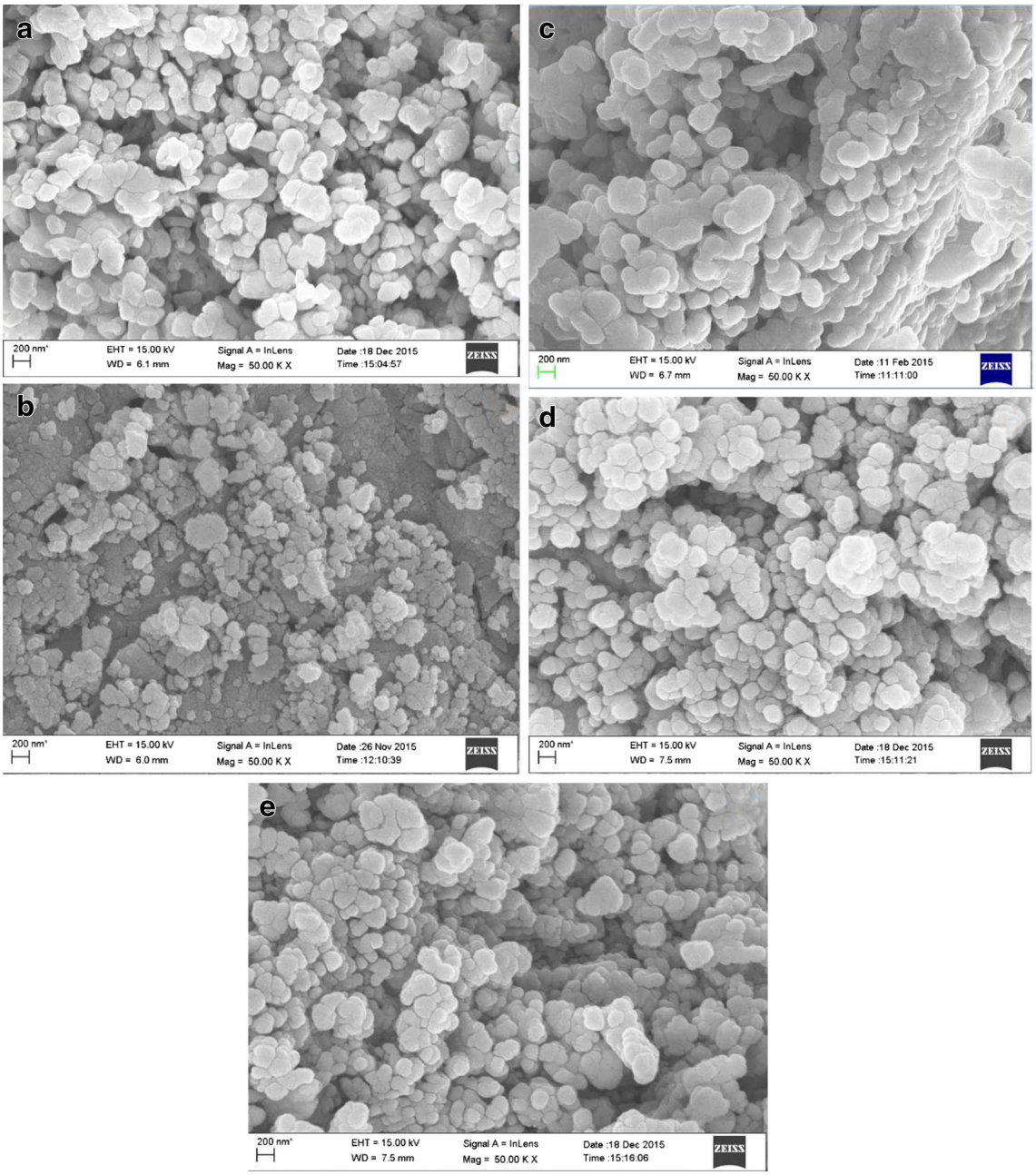

Fig. 2 SEM images of $Sr_{1-x}La_xFe_{12}O_{19}$: **a** $x = 0.0$, **b** $x = 0.10$, **c** $x = 0.15$, **d** $x = 0.20$, and **e** $x = 0.25$

Table 2 The effect of La substitution on magnetic properties of $Sr_{1-x}La_xFe_{12}O_{19}$ ($x = 0.0$, 0.10, 0.15, 0.20, and 0.25) ferrites

x	0.00	0.10	0.15	0.20	0.25
M_s (emu/g)	65.36	62.3	60.6	56.34	57.85
H_c(Oe)	5059	5791	5692	5683	5661
M_r (emu/g)	37.1	36.2	34.3	32.12	32.95
H_a (kOe)	11.8	14.2	14.2	13.8	13.2
M_r/M_s	0.568	0.566	0.566	0.57	0.57
D_m (nm)	187	148	160	180	180

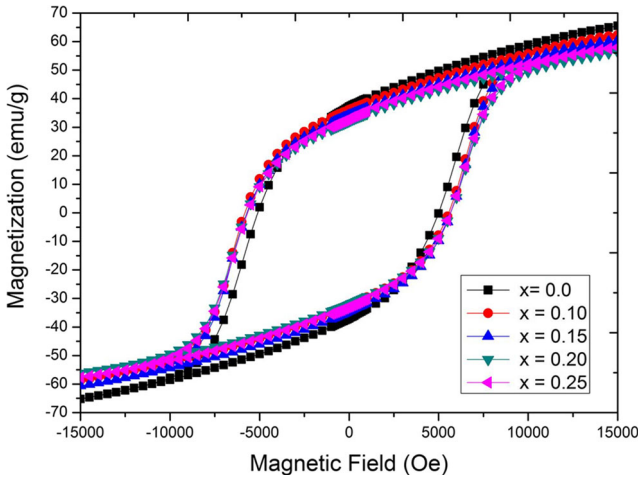

Fig. 3 Hysteresis loops (M vs. H) of $Sr_{1-x}La_xFe_{12}O_{19}$ ($x = 0.0$, 0.10, 0.15, 0.20, and 0.25) ferrites

$x = 0.25$ sample. The variation of permittivity with frequency arises mainly due to the interfacial polarization and intrinsic electric dipole polarization. The interfacial polarization results from the heterogeneous structure of ferrites comprising well-conducting grains separated by poorly conducting grain boundaries as proposed by Koops [20]. The ε'' values show one or two peaks for all the compositions. The maximum obtained values of ε'' at resonance peaks in 12.4–18 GHz frequency range are 0.93, 1.30, 3.16, 1.67, and 2.10 for the composition $x = 0.0$, 0.10, 0.15, 0.20, and 0.25, respectively. It is known that resonance peaks are usually attributed to polarization [21]. Substitution of La^{3+} is expected to convert some of the Fe^{3+} to Fe^{2+} in the ferrite in order to maintain charge neutrality. The electron hopping between Fe^{3+} and Fe^{2+} enhances the ε'', and also, the excess Fe^{2+} strengthens the interfacial polarization in ferrites [22].

The real-part μ' and imaginary-part μ'' of permeability have shown a dispersion relation with increase in frequency, exhibiting magnetic resonance (Fig. 4c, d). The maximum values of μ' of the lanthanum-doped samples are higher than those of the unsubstituted sample. The permeability of polycrystalline ferrites can be described as the superposition of two different magnetizing mechanisms: domain wall motion and domain spin rotation [23]. The real-part permeability can be expressed as $\mu' = 1+$ spin rotational susceptibility (χ_{spin}) + domain wall susceptibility (χ_{domain}). The χ_{spin} and χ_{domain} in turn are related to the square of saturation

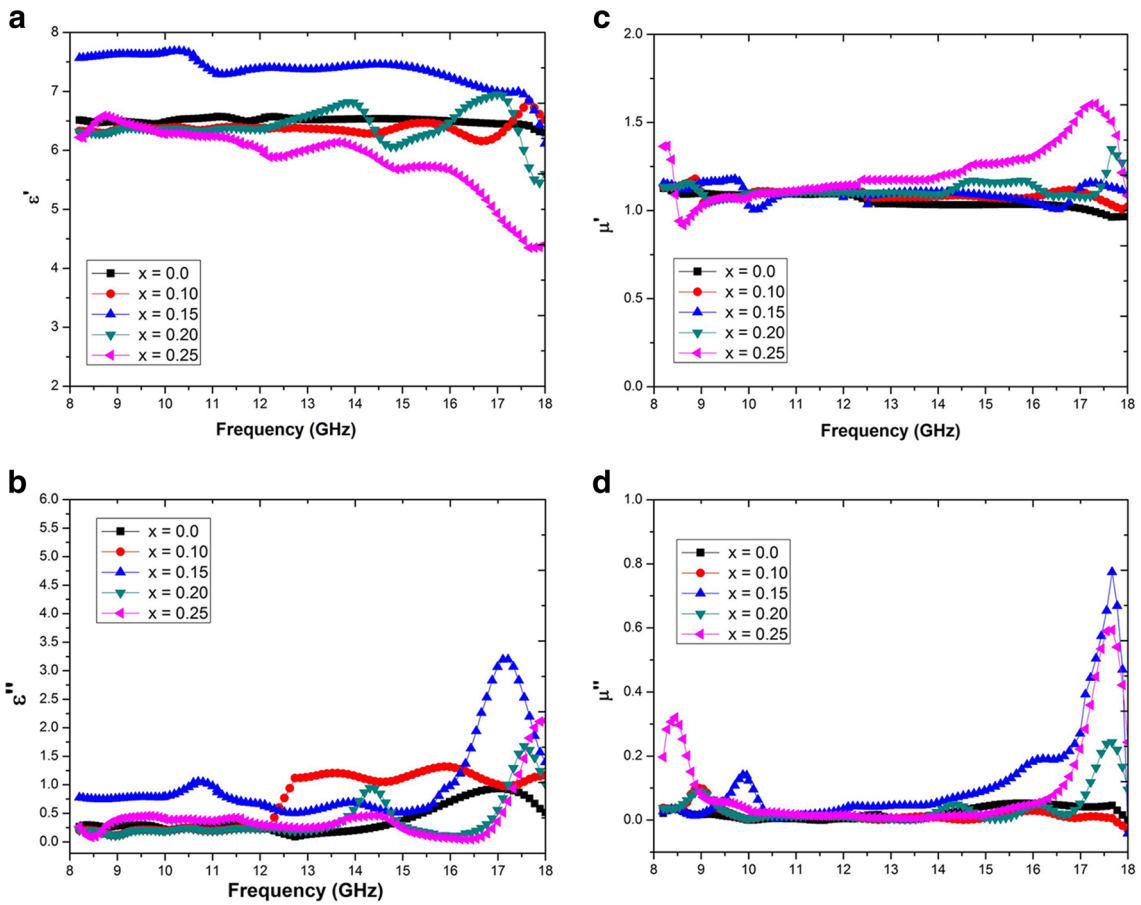

Fig. 4 Variations of **a** ε', **b** ε'', **c** μ', and **d** μ'' with frequency and substitution in $Sr_{1-x}La_xFe_{12}O_{19}$

M_s [24]. Hence, a higher value of M_s is one of the reasons for an improved value of μ' for the La^{3+}-substituted strontium ferrite. The peaks in the spectra of μ'' express the energy absorption. The maximum obtained values of μ'' in 8–18 GHz frequency range are 0.052, 0.029, 0.77, 0.29, and 0.25 for $x = 0.0$, 0.10, 0.15, 0.20, and 0.25, respectively. The values of μ' and μ'' indicate that the La^{3+} doping in strontium ferrite has improved the magnetic loss in the Ku band.

The microwave absorption of ferrite material is characterized by tanδ (gross loss tangent): $\tan\delta = \tan\delta_e + \tan\delta_m = \varepsilon''/\varepsilon' + \mu''/\mu'$, where $\tan\delta_e$ is the dielectric loss tangent and $\tan\delta_m$ is the magnetic loss tangent. Figure 5 shows the gross loss tangent of $Sr_{1-x}La_xFe_{12}O_{19}$ ($x = 0.0$, 0.10, 0.15, 0.20, and 0.25). The larger value of the tanδ, the better will be the microwave-absorbing properties of the material. In the X band, $x = 0.25$ and 0.15 compositions have observed comparatively high values of gross loss tangent (0.33 and 0.22). In the Ku band, the maximum obtained values of tanδ are 0.18, 0.24, 0.85, 0.46, and 0.84 for composition x, which is equal to 0.0, 0.10, 0.15, 0.20, and 0.25, respectively. Both dielectric and magnetic losses contribute to gross tangent loss in the Ku band with La^{3+} substitution in strontium ferrite.

The reflection loss (RL) curves were determined from the complex relative permittivity (ε_r), complex relative permeability (μ_r) at a given frequency (f), absorber thickness (t), velocity of electromagnetic waves in free space (c), and input impedance (Z_{in}) of metal-backed with the following equations [25]:

$$Z_{in} = Z_0 (\mu_r/\varepsilon_r)^{1/2} \tanh\left(j\left(2\pi f t (\mu_r \varepsilon_r)^{1/2}\right)/c\right) \text{ and RL (dB)} = 20 \log\left((Z_{in} - 1)/(Z_{in} + 1)\right)$$

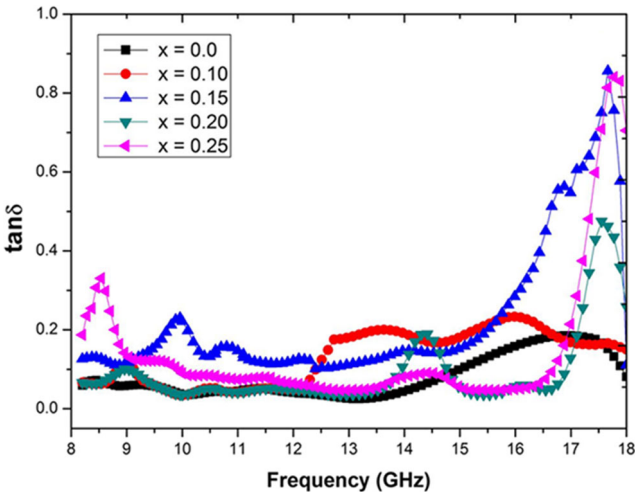

Fig. 5 Variations of tanδ with frequency and substitution in $Sr_{1-x}La_xFe_{12}O_{19}$

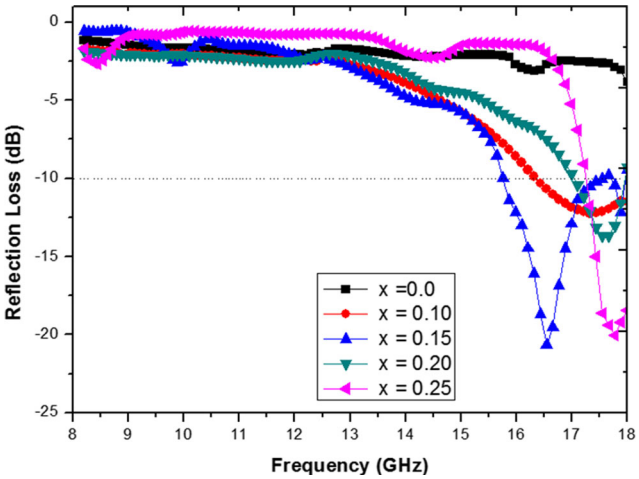

Fig. 6 Reflection loss of $Sr_{1-x}La_xFe_{12}O_{19}$ in 8–18 GHz frequency

Figure 6 shows the variation of reflection loss vs. frequency observed in 1.6-mm-thick La^{3+}-doped strontium ferrite with $x = 0.0$, 0.10, 0.15, 0.20, and 0.25 in 8–18 GHz. The bandwidth of pure hexagonal ferrite is relatively small to be used as a microwave absorber material, and its absorption characteristic is in higher-frequency range around 45 GHz [26, 27]. For a sample with $x = 0.10$, the minimum reflection loss value of -12.24 dB is observed at 17.43 GHz. The minimum reflection loss value increases from -12.24 dB in the sample with $x = 0.10$ to -20.66 dB in the sample with $x = 0.15$ at 16.5 GHz. The bandwidth that can be covered by the sample with $x = 0.15$ is about 2.1 GHz. The minimum reflection loss of -13.78 and -20.19 dB are observed for $x = 0.20$ and $x = 0.25$ samples, respectively. The result of reflection loss is in accordance with the maximum obtained values of the gross loss tangent. Finally, it should be noticed that the main absorption mechanism in these samples is due to both the dielectric and magnetic properties in the Ku band.

4 Conclusion

A series of morphologically pure $Sr_{1-x}La_xFe_{12}O_{19}$ ferrites has been successfully prepared by auto-combustion method at a temperature of 1100 °C for 5 h. The crystallite size of samples is in between 34.3 and 42.56 nm. The saturation magnetization has decreased, whereas coercivity has increased with lanthanum substitution as compared with the undoped strontium ferrite. The gross loss tangent has shown an improvement with La^{3+} substitution in strontium ferrite. These lanthanum-doped strontium ferrites show a reflection loss of more than 90 % in the Ku band. The observed results suggest that these synthesized ferrites have potential

applications as single-layer microwave absorbers for EMI suppression.

References

1. Cho, H., Kim, S.: M-hexaferrites with planer magnetic anisotropy and their application to high-frequency microwave absorbers. IEEE Trans. Magn. **35**, 3151–3153 (2002)
2. Singh, C., Narang, S.B., Hudiara, I.S., Sudheendran, K., Raju, K.C.J.: Complex permittivity and complex permeability of Sr ions substituted Ba ferrite at X-band. J. Magn. Magn. Mater. **320**, 1657–1665 (2008)
3. Narang, S.B., Kaur, P., Bahel, S., Singh, C.: Microwave characterization of Co-Ti substituted barium hexagonal ferrites in X-band. J. Magn. Magn. Mater. **405**, 17–21 (2016)
4. Jamalian, M., Ghasemi, A., Paimozd, E.: Sol–gel synthesis of Mn–Sn–Ti-substituted strontium hexaferrite nanoparticles: structural, magnetic and reflection-loss properties. J. Electron. Mater. **43**, 1076–1082 (2014)
5. Iqbal, M.J., Ashiq, M.N., Gomez, P.H., Munzor, J.M.: Synthesis, physical, magnetic and electrical properties of Al–Ga substituted co-precipitated nanocrystalline strontium hexaferrite. J. Magn. Magn. Mater. **320**, 881–886 (2008)
6. Lee, J.H., Kim, H.S., Won, C.W.: Magnetic properties of strontium ferrite powder made by hydrothermal processing. J. Mater. Sci. Lett. **15**, 295–297 (1996)
7. Sharbati, A., Choopani, S., Azar, A.M., Senna, M.: Structure and electromagnetic behavior of nanocrystalline $SrMg_xZr_xFe_{12-2x}O_{19}$ in the 8–12 GHz frequency range. J. Solid State Commun. **150**, 2218–2222 (2010)
8. Iqbal, M.J., Ashiq, M.N., Gomez, P.H.: Effect of doping of Zr–Zn binary mixtures on structural, electrical and magnetic properties of Sr-hexaferrite nanoparticles. J. Alloys Compd. **478**, 736–740 (2009)
9. Rai, B.K., Mishra, S.R., Nguyen, V.V., Liu, J.P.: Influence of RE3+ co-substitution on the structure and magnetic properties of $Sr_{0.82}RE_{0.18}Fe_{12}O_{19}$ (RE: $La_{0.18-x}Pr_x$) ferrites. J. Alloys Compd. **581**, 275–281 (2013)
10. Chen, N., Yang, K., Gu, M.Y.: Microwave absorption properties of La-substituted M-type strontium ferrites. J. Alloys Compd. **490**, 609–612 (2010)
11. Deng, L., Ding, L., Zhou, K., Huang, S., Hu, Z., Yang, B.: Electromagnetic properties and microwave absorption of W-type hexagonal ferrites doped with La^{3+}. J. Magn. Magn. Mater. **323**, 1895–1898 (2011)
12. Cullity, B.D. Elements of X-ray diffraction, 2nd edn. Addison-Wesley, Reading (1978)
13. Teh, G.B., Wong, Y.C., Tilley, R.D.: Effect of annealing temperature on the structural, photoluminescence and magnetic properties of sol–gel derived magnetoplumbite-type (M-type) hexagonal strontium ferrite. J. Magn. Magn. Mater. **323**, 2318–2322 (2011)
14. Scherrer, P.: Nachr. Ges. Wiss. Gottingen. **26**, 98–100 (1918)
15. Went, J.J., Rathenau, G.W., Gorter, E.W., van Oosterhout, G.W.: Hexagonal iron-oxide compounds as permanent-magnet materials. Phys. Rev. **86**, 424 (1952)
16. Kumar, N., Kumar, A., Jha, R., Dogra, A., Pasricha, R., Kotnala, R.K., Kishan, H., Awana, V.P.S.: Impact of particle size on room temperature ferrimagnetism of $SrFe_{12}O_{19}$. J. Supercond. Nov. Magn. **23**, 423–427 (2010)
17. Wang, S., Ding, J., Shi, Y., Chen, Y.J.: High coercivity in mechanically alloyed $BaFe_{10}Al_2O_{19}$. J. Magn. Magn. Mater. **219**, 206–212 (2000)
18. Singh, C., Narang, S.B., Hudiara, I.S., Bai, Y.: The effect of Co and Zr substitution on dc magnetic pr operties of Ba–Sr ferrite. J. Alloys Compd. **464**(1), 429–433 (2008)
19. Dho, J., Lee, E.K., Park, J.Y., Hur, N.H.: Effects of the grain boundary on the coercivity of barium ferrite $BaFe_{12}O_{19}$. J. Magn. Magn. Mater. **285**, 164–168 (2005)
20. Koops, C.G.: On the dispersion of resistivity and dielectric constant of some semiconductors at audio frequencies. Phys. Rev. **83**, 121–124 (1951)
21. Ni, S., Wang, X., Zhou, G., Yang, F., Wang, J., He, D.: Designed synthesis of wide range microwave absorption Fe_3O_4–carbon sphere composite. J. Alloys. Compd. **489**, 252–256 (2010)
22. Liu, X.G., Li, B., Geng, D.Y., Cui, W.B., Yang, F., Xie, Z.G., et al.: (Fe, Ni)/C nanocapsules for electromagnetic-wave-absorber in the whole Ku-band. Carbon **47**(2), 470–474 (2009)
23. Wang, C., Li, L., Zhou, J., Qi, X., Yue, Z., Wang, X.: Microstructures and high frequency magnetic properties of low-temperature sintered Co-Ti substituted barium ferrites. J. Magn. Magn. Mater. **257**, 100–106 (2003)
24. Nakamura, T.: Low temperature sintering of Ni-Zn-Cu ferrites and their permeability spectra. J. Magn. Magn. Mater. **168**, 285–291 (1996)
25. Ghasemi, A.: Enhanced reflection loss and permittivity of self assembled Mg–Co–Zr substituted barium ferrite dot array on carbon nanotube. J. Magn. Magn. Mater. **324**(6), 1080–1083 (2012)
26. Choopani, S., Keyhan, N., Ghasemi, A., Sharbati, A., Alam, R.S.: Structural, magnetic and microwave absorption characteristics of $BaCo_xMn_xTi_{2x}Fe_{12-4x}O_{19}$. Mater. Chem. Phys. **113**(2–3), 717–720 (2009)
27. Ghasemi, A., Liu, X., Morisako, A.: Magnetic and microwave absorption properties of $BaFe_{12-x}(Mn_{0.5}Cu_{0.5}Zr)_{x/2}O_{19}$ synthesized by sol–gel processing. J. Magn. Magn. Mater. **316**, e105–e108 (2007)